EUROPHYSICS LETTERS 15 May 1999

Europhys. Lett., **46** (4), pp. 419-424 (1999)

Minima and maxima of the local density of states for one-dimensional periodic systems

A. Moroz(*)

FOM-Instituut voor Atoom- en Molecuulfysica
Kruislaan 407, 1098 SJ Amsterdam, The Netherlands

(received 14 December 1998; accepted in final form 11 March 1999)

PACS. 03.40Kf – Waves and wave propagation: general mathematical aspects.
PACS. 42.70Qs – Photonic bandgap materials.

Abstract. – An analytic expression for the Green function of the one-dimensional periodic Helmholtz operator is used to analyze the behaviour of the local density of states (LDOS). We provide numerical evidence that in the n-th band the LDOS has at least n minima and maxima. Near the band edge ω_c, the LDOS exhibits strong fluctuations, with its mimima approaching zero and the maxima diverging to infinity. For the lowest band, the ratio of the maximum to the minimum of the LDOS is shown to diverge as $(\omega_c - \omega)^{-1}$ as ω approaches the band edge. Since, in the case of electromagnetic waves, the LDOS governs the spontaneous emission of light of embedded atoms and molecules, this may have profound implications for technology using photonic crystals.

In this letter, we study the one-dimensional periodic Helmholtz equation

$$[\triangle + \varepsilon(\mathbf{x})\omega^2]\,\psi(\mathbf{x}) = 0, \tag{1}$$

where $\triangle$ is the Laplacian, $\varepsilon(\mathbf{x})$ is some real positive periodic function of the coordinate $\mathbf{x} \in \mathbb{R}$, $\varepsilon(\mathbf{x}) \geq \delta > 0$, and ω and ψ are the eigenvalue and the eigenfunction, respectively, to be calculated. In order to illustrate the main features of the general case [1], we specialize to the so-called constant muffin-tin case, in which case $\varepsilon(\mathbf{x})$ is assumed to be a piece-wise constant and taking on two values ε_b and ε_s. The constant muffin-tin case can also be viewed as the Helmholtz analogue of the Kronig-Penney model [2]. Already at this level, the Helmholtz equation plays an important role in a number of different physical situations involving propagation of acoustic and elastic waves [3]. Since in one dimension or at normal incidence on a stratified medium, Maxwell's equations coincide with the Helmholtz equation, the latter also describes several physically interesting and important situations involving propagation of light at normal incidence in stratified media [4]. Examples include grating-like structures, cylindrical cavities [5], and the so-called one-dimensional photonic crystals [6]. For

(*) http://www.amolf.nl/external/wwwlab/atoms/theory/

these applications, ω in eq. (1) is the angular frequency divided by a characteristic speed of propagation in a medium, and $\varepsilon(\mathbf{x})$ is the dielectric constant.

As in the Schrödinger case, the spectrum of the periodic Helmholtz equation (1) consists of frequency bands separated by spectral gaps. To find the Green function, the Helmholtz equation (1) is considered here as a generalized eigenvalue problem [7]. One studies the properties of an operator $H = \varepsilon^{-1}\triangle$ in the Hilbert space $L^2(\mathbb{R}, \varepsilon(\mathbf{x})\mathrm{d}\mathbf{x})$ (cf. eq. (VII-6.2) of [7]), in which the scalar product is defined as $(f,g) = \int \varepsilon f^* g \,\mathrm{d}\mathbf{x}$ [8]. This formulation seems to be more convenient for adapting a general on-shell multiple-scattering theory (MST), as originally developed for the Schrödinger equation [9], to the case of the Helmholtz equation (1) and more generally to Maxwell's equations [8] than that used in [10]. The reason is that the solutions $f \in L^2(\mathbb{R}, \varepsilon(\mathbf{x})\mathrm{d}\mathbf{x})$ are required to satisfy the conventional boundary conditions: they are, together with their derivatives, continuous at discontinuities of $\varepsilon(\mathbf{x})$. (In the case of Maxwell's equation, the continuity holds for the appropriate normal and tangential field components.)

Given $H = \varepsilon^{-1}\triangle$, the resolvent is defined in the generalized sense as $G(z) = (z - H)^{-1}$ (cf. eq. (VII-6.8) of [7]). The Green function $G(\mathbf{x},\mathbf{x})$ at a given frequency ω is then defined as the limit

$$G(\omega;\mathbf{x},\mathbf{x}) = \lim_{t\to+0} \langle\, \mathbf{x} \,|\, [(\omega + it)^2 - H]^{-1} \,|\, \mathbf{x} \,\rangle\,. \tag{2}$$

Then, formally,

$$\mathrm{Im}\, G(\omega;\mathbf{x},\mathbf{x}) = -\pi\, \langle\, \mathbf{x} \,|\, \delta(\omega^2 - H) \,|\, \mathbf{x} \,\rangle. \tag{3}$$

Our main goal is to investigate the properties of the local density of states (LDOS) [8]

$$n(\omega,\mathbf{x}) = -\frac{2\omega}{\pi}\, \mathrm{Im}\, G(\omega;\mathbf{x},\mathbf{x}). \tag{4}$$

The prefactor 2ω originates from the fact that the analog of the energy E used in the Schrödinger equation is $E = \omega^2$ and hence $\mathrm{d}E = 2\omega\mathrm{d}\omega$. The DOS $n(\omega)$ and the integrated DOS $N(\omega)$ per primitive cell are defined as

$$n(\omega) = \int_{\mathrm{WS}} n(\omega,\mathbf{x})\,\mathrm{d}\mathbf{x}, \qquad N(\omega) = \int_{-\infty}^{\omega} n(t)\,\mathrm{d}t, \tag{5}$$

where the subscript WS stands for the integration over the primitive (Wigner-Seitz) cell. According to its definition, $N(\omega)$ describes the number of modes per primitive lattice cell with $\omega' \le \omega$ and $\mathrm{d}N(\omega) = n(\omega)\,\mathrm{d}\omega$.

Although there exists an enormous amount of literature on one-dimensional periodic systems (see, for example, [11] for references), little is known about the properties of the LDOS. Interest in the LDOS has increased dramatically in recent years with the advent of photonic crystals [12], *i.e.*, dielectrics with a periodic dielectric constant. It was shown, both in a scalar approximation [13] and for the full Maxwell equations [14], that the spontaneous emission (SE) rate Γ of atoms and molecules embedded in a photonic crystal is directly proportional to the LDOS,

$$\Gamma(\mathbf{x}) = \frac{2\pi|\mu_{ab}|^2}{\hbar}\frac{n(\omega,\mathbf{x})}{\varepsilon(\mathbf{x})} = -\frac{4\omega|\mu_{ab}|^2}{\hbar}\,\frac{\mathrm{Im}\, G(\omega;\mathbf{x},\mathbf{x})}{\varepsilon(\mathbf{x})}, \tag{6}$$

where μ_{ab} is the dipole moment of the optical transition. Therefore, the spontaneous emission can either be reduced down to zero (at zeroes of $n(\omega,\mathbf{x})$) or substantially enhanced (at points which correspond to the maxima of $n(\omega,\mathbf{x})$) with respect to the vacuum case. Suppression of the SE may have applications for semiconductor lasers, solar cells, heterojunction bipolar transistors, and thresholdless lasers [12]. On the other hand, the enhancement of the SE is a way to create new sources of light for ultra-fast optical communication systems [5, 6]. Thus far, the main focus for suppressing $n(\omega, \mathbf{x})$ was to achieve a photonic band-gap, *i.e.*, by opening an interval I_g in the frequency region for which $n(\omega) = 0$. Unfortunately, satisfying the condition for infrared or visible frequencies in three dimensions turns out to be extremely difficult. Therefore, a natural question arises [15] whether, for frequencies within a band (*i.e.*, for $n(\omega) \neq 0$), one can find points in the lattice cell for which $n(\omega, \mathbf{x})$ is strongly modified with respect to its vacuum value.

Results. – In our case, the Green function in (3) can be calculated analytically by adapting the first-principle on-shell multiple-scattering theory (MST) as originally employed for the Schrödinger equation [9,16]. The unique feature of the on-shell MST is that, for nonoverlapping (muffin-tin) scatterers [9] (the present situation), it disentangles single-scattering and multiple-scattering effects (see [17] for a recent discussion) and the expressions for the Green function and scattering matrices involve only the single-scatterer phase shifts and a lattice sum (also called the structure constant) [9]. Here, we only present our main results. Details of our calculation will appear elsewhere [1]. For results on the band structure and the DOS for the three-dimensional photonic crystal of dielectric spheres using this approach see [18].

In the following we expand on the work of Butler [16]. Without any loss of generality, we shall assume that $\varepsilon_s > \varepsilon_b$. We call a scatterer the region with $\varepsilon(\mathbf{x}) = \varepsilon_s$ and isolated on its both sides by regions with $\varepsilon(\mathbf{x}) = \varepsilon_b$. Let us choose our coordinate axis such that the origin corresponds to the center of a scatterer. Let the center of a scatterer be also the center of a primitive cell. Within the frequency band, the Green function is purely imaginary [19], *i.e.*, $\mathrm{Re}G(\mathbf{x}, \mathbf{x}) = 0$, and in the central cell we have

$$\mathrm{Im}\, G(\omega; \mathbf{x}, \mathbf{x}) = -\varepsilon(\mathbf{x}) \sum_{l=0}^{1} \frac{|R_l(r)|^2}{2\sigma\sqrt{1-s^2}} \frac{\sin(\sigma a + 2\eta_{1-l})}{\cos^2(\eta_0 - \eta_1)}, \tag{7}$$

where R_l is a particular real solution of (1) in the presence of a single scatterer,

$$R_l(r) = \begin{cases} C_l j_l(\rho r), & r < r_s, \\ j_l(\sigma r)\cos\eta_l - n_l(\sigma r)\sin\eta_l, & r > r_s, \end{cases} \tag{8}$$

and $s = \cos(\sigma a + \eta_0 + \eta_1)/\cos(\eta_0 - \eta_1)$. (Within a band, $|s| \leq 1$ and the dispersion relation is determined by the equation $\cos \mathbf{k}a = s$, where $\mathbf{k}$ is the Bloch momentum.) Here $r = |\mathbf{x}|$, a is the lattice constant, *i.e.*, the length of the primitive cell, $\rho = \omega\sqrt{\varepsilon_s}$, $\sigma = \omega\sqrt{\varepsilon_b}$, $j_0(x) = \cos x$, $j_1(x) = \sin x$, $n_0(x) = \sin x$, $n_1(x) = -\cos x$, η_l is a phase shift, and C_l is a constant. The latter two are determined by the relations

$$\begin{aligned} C_l &= \begin{cases} \left[1 + (p^2 - 1)\sin^2 \rho r_s\right]^{-1/2}, & l = 0, \\ \left[1 + (p^2 - 1)\cos^2 \rho r_s\right]^{-1/2}, & l = 1, \end{cases} \\ \cos\eta_0 &= C_0\left[\cos\sigma r_s \cos\rho r_s + p\,\sin\sigma r_s \sin\rho r_s\right], \\ \sin\eta_0 &= C_0\left[-\sin\sigma r_s \cos\rho r_s + p\,\cos\sigma r_s \sin\rho r_s\right], \\ \cos\eta_1 &= C_1\left[\sin\sigma r_s \sin\rho r_s + p\,\cos\sigma r_s \cos\rho r_s\right], \\ \sin\eta_1 &= C_1\left[\cos\sigma r_s \sin\rho r_s - p\,\sin\sigma r_s \cos\rho r_s\right], \end{aligned}$$

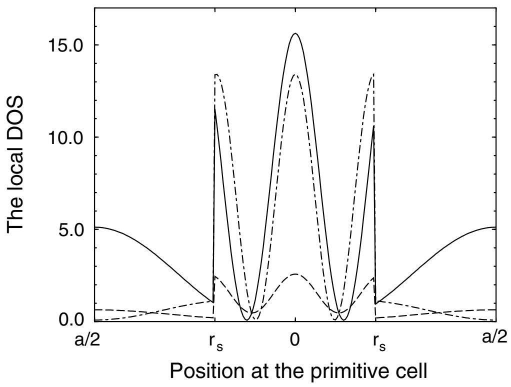

Fig. 1

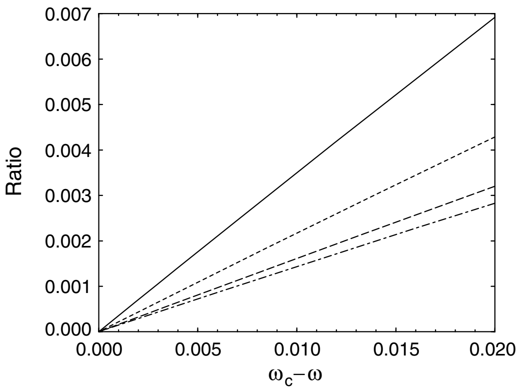

Fig. 2

Fig. 1. – The local DOS within the third band for $\varepsilon_b = 1$, $\varepsilon_s = 12$, and $r_s = 0.2a$. The solid line is for $\omega = 3.7561$ near the lower band edge, the dot-dashed line is for $\omega = 4.6081$ near the upper band edge. For comparison, also the profile of the LDOS near the third band center at $\omega = 4.1821$ is shown (long-dashed line).

Fig. 2. – The ratio of the minimum to the maximum of the local density of states (the inverse of χ) within the first band decreases linearly with the distance to the band edge. We have plotted here different (ε_s, r_s) configurations with $\varepsilon_b = 1$ fixed, namely, $(6, 0.2a)$ (solid line), $(12, 0.2a)$ (dashed line), $(12, 0.1a)$ (long-dashed line), and $(24, 0.2a)$ (dot-dashed line).

where $p = \sqrt{\varepsilon_s/\varepsilon_b}$. The LDOS is then obtained by plugging (7) into (4). One can verify [1] that the DOS obtained according to (5) coincides with the DOS obtained from the dispersion relation $k = k(\omega)$,

$$n(\omega) = \frac{a}{\pi}\left|\frac{\mathrm{d}k}{\mathrm{d}\omega}\right| . \tag{9}$$

The fact that eqs. (5) and (9) give the same result for $n(\omega)$ can be straighforwardly verified in the limiting case $r_s \to 0$ and $\varepsilon_s \to \infty$, provided that $2\varepsilon_s r_s \to \lambda\varepsilon_b$. The limit corresponds to a Helmholtz analogue of the Kronig-Penny model and is described by

$$\varepsilon(\mathbf{x}) = \varepsilon_b\left[1 + \lambda\sum_{m=-\infty}^{\infty}\delta(\mathbf{x} - am)\right] . \tag{10}$$

In the limit, the solutions R_l are continuous, $C_0 = [1 + \lambda^2\sigma^2/4]^{-1/2}$, $C_1 = 0$, $\cos\eta_0 = C_0$, $\sin\eta_0 = \lambda\sigma C_0/2$, and $\eta_1 = 0$.

Being a periodic function of $\mathbf{x}$, $n(\omega, \mathbf{x})$ takes on a number of local maxima and minima within a primitive cell. Generally speaking, the number of maxima within the scattering region equals the number of a band when ordered from the lowest one, *i.e.*, there is one maximum in the lowest band, etc. In the lowest band, the maximum appears at the center of a scatterer while the minimum appears at the primitive cell boundary. This conforms to an intuitive picture of standing waves near the band edges as discussed by Russell [20]. However, for higher bands, it contradicts conventional wisdom which says, for example, that within the second band $n(\omega, \mathbf{x})$ is concentrated in regions with the lower dielectric constant [20]. According to our calculation, all maxima of $n(\omega, \mathbf{x})$ appear within the scatterer, *i.e.*, in the regions with the higher dielectric constant (see fig. 1). However, there is one subtle point. An additional maximum appears at the primitive cell boundary for frequencies near the lower band edge. As frequency increases towards the upper band edge, this maximum turns gradually into a minimum with $n(\omega, \mathbf{x})$ approaching zero. It is rather interesting to see that positions of the maxima and minima hardly change within a given band (see fig. 1).

One knows that at the band edge ω_c, $n(\omega)$ diverges as $|\omega_c - \omega|^{-1/2}$ (van Hove peaks). This does not mean, however, that $n(\omega, \mathbf{x})$ increases for a given $\mathbf{x}$ as $\omega \to \omega_c$. On the contrary, the mimima of $n(\omega, \mathbf{x})$ deepen and approach zero while the maxima of $n(\omega, \mathbf{x})$ diverge to infinity. Obviously, the ratio χ of a maximum to minimum of the LDOS within a primitive cell diverges as well. In the lowest band, this ratio can be expressed entirely in terms of boundary values of $R_l(r)$,

$$\chi = \frac{\varepsilon_s G(0,0)}{\varepsilon_b G(a/2, a/2)} = \frac{R_1^2(a/2)\gamma_1(|\gamma_1| + |\gamma_0|)}{C_1^2 \varepsilon_b \omega^2}, \tag{11}$$

where $\gamma_l = R_l'/R_l$ are logarithmic derivatives at the cell boundary, with prime indicating derivative with respect to r. We found that χ diverges as $(\omega_c - \omega)^{-1}$ when $\omega \to \omega_c$ (see fig. 2).

Conclusions. – To conclude, our results may have a profound impact on an existing paradigm in enhancing SE. The latter suggests to create a defect in an otherwise perfect crystal, which, under certain conditions, induces a defect (impurity) level within a frequency gap [5, 6]. The impurity level then serves as a cavity the quality factor of which increases exponentially with the size (the number of periods) of a (finite) crystal. Based on the DOS within a cavity one can estimate the SE enhancement factor [21]. Experimentally, the highest SE enhancement factor achieved thus far is 35 [6]. Our results show that creating a localized defect mode in a crystal is not the only way to enhance the SE. Indeed, the enhancement factor was shown to diverge at certain points of the primitive cell even in a perfect crystal for frequencies within a band near band edges (see fig. 2). As a band edge is approached, every primitive cell turns out to be a resonant cavity (see [1] for more details). For practical purposes it is interesting to know that positions of the maxima and minima of the LDOS within a primitive cell hardly change with frequency within a given band (see fig. 1) and that their number within the scattering region equals the number of a band when ordered from the lowest one. Thus, by judiciously positioning the impurity atom within the primitive cell, one can achieve strong modulation of its SE characteristics. Indeed, at a maximum of the LDOS for frequencies within a band as far as 10% below the band edge, the SE enhancement factor can be as large as ≈ 100. These results are directly relevant to quantum optical experiments in which atoms, dye molecules, or other active materials are inserted into specific locations within the photonic crystal. The changes in the SE can be observed, for example, in a stratified (layered) dielectric medium in a setup where the impurity atom is excited by a laser beam parallel to the planes of stratification and the detection of SE is performed in normal direction.

***

I should like to thank Drs. A. van Blaaderen, H. J. Hopman, C. Rella, and A. Tip for careful reading of the manuscript and useful comments, and Prof. W. H. Butler for discussion. This work is part of the research program by the Stichting voor Fundamenteel Onderzoek der Materie (Foundation for Fundamental Research on Matter) which was made possible by financial support from the Nederlandse Organisatie voor Wetenschappelijk Onderzoek (Netherlands Organization for Scientific Research).

REFERENCES

[1] Moroz A., in preparation.
[2] Kronig R. L. and Penney W. G., *Proc. R. Soc. London, Ser. A*, **20** (1931) 499.
[3] Morse P. M. and Feshbach H., *Methods of Theoretical Physics* (Mc Graw Hill, New York) 1953, Part II, Secs. XI, XIII.
[4] Abelès F., *Ann. Phys. (Paris)*, **5** (1950) 596, 603, 706, 777; Born M. and Wolf E., *Principles of Optics*, 3rd edition (Pergamon Press, Oxford) 1964, Chapt. 1.6.
[5] Rigby P. and Krauss T. F., *Nature*, **390** (1997) 125.
[6] Foresi J. S. *et al.*, *Nature*, **390** (1997) 143.
[7] Kato T., *Perturbation Theory for Linear Operators* (Springer, New York) 1966.
[8] Moroz A., *Phys. Rev. B*, **51** (1995) 2068; Moroz A., in *Confined Electrons and Photons: New Physics and Applications*, edited by E. Burstein and C. Weisbuch (Plenum Press, New York) 1995, p. 741.
[9] Beeby J. L., *Proc. R. Soc., London, Ser. A*, **279** (1964) 82.
[10] Dorren H. J. S. and Tip A., *J. Math. Phys.*, **32** (1991) 3060.
[11] Eastham M. S. P., *The Spectral Theory of Periodic Differential Equations* (Scottish Academy Press, Edinburgh-London) 1973; Reed M. and Simon B., *Analysis of Operators* (Academic Press, New York) 1978, Sec. XIII.16 and references on pp. 358-360; Albeverio S., Gesztesy F., Hoegh-Krohn R. and Holden H., *Solvable Models in Quantum Mechanics* (Springer, New York) 1988.
[12] Bykov V. P., *Sov. J. Quantum Electron.*, **4** (1975) 861; Yablonovitch E., *Phys. Rev. Lett.*, **58** (1987) 2059; John S., *Phys. Rev. Lett.*, **58** (1987) 2486.
[13] Sprik R., van Tiggelen B. A. and Lagendijk A., *Europhys. Lett.*, **35** (1996) 265.
[14] Glauber R. J. and Lewenstein M., *Phys. Rev. A*, **43** (1991) 467, eq. (6.12); Tip A., *Phys. Rev. A*, **56** (1997) 5022; **57** (1998) 4818.
[15] Busch K. and John S., *Phys. Rev. E*, **58** (1998) 3896.
[16] Butler W. H., *Phys. Rev. B*, **14** (1976) 468.
[17] Moroz A. and Tip A., *Phys. Lett. A*, **235** (1997) 195.
[18] Moroz A. and Sommers C., *J. Phys.: Condens. Matter*, **11** (1999) 997; Moroz A. and Tip A., *J. Phys. Condens. Matter*, **11** (1999) 2503; Moroz A., *A simple formula for the L-gap width of a face-centered-cubic photonic crystal*, submitted for publication.
[19] Thouless D. J., *J. Phys.: Solid State*, **5** (1972) 77.
[20] Russell P. St. J., *Physics World*, August issue (1992) 37; Joannopoulos J. D., Maede R. D. and Winn J. N., *Photonic Crystals: Molding the Flow of Light* (Princeton University Press) 1995.
[21] Yokoyama H. and Brorson S. D., *J. Appl. Phys.*, **66** (1989) 4801.